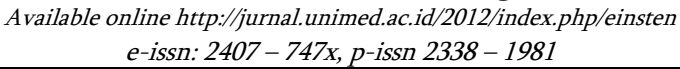


EINSTEIN (e-Journal)

Jurnal Hasil Penelitian Bidang Fisika





GREEN-SYNTHESIZED FE3O4/TIO2 ADSORPTION MATERIAL VIA COPRECIPITATION METHOD USING MORINGA OLEIFERA LEAF EXTRACT FOR THE DEGRADATION OF METHYLENE BLUE

Ridwan Yusuf Lubis¹, Abdul Halim Daulay², Masthura³

Physics Department, Universitas Islam Negeri Sumatera Utara, Indonesia <u>ridwanyusuflubis@uinsu.ac.id</u>

Submit: August 2025. Approved: September 2025. Published: October 2025.

ABSTRACT

Iron sand can be utilized as a raw material for the synthesis of Fe3O4 nanomaterials, which can be applied in various technologies such as wastewater treatment. The Fe3O4/TiO2 photocatalyst material was synthesized using the coprecipitation method with variations of FTMO2:1, FTMO1:1, and FTMO1:2, combined with Moringa oleifera leaf extract. The synthesized Fe3O4 powder from iron sand was mixed with TTIP and the leaf extract solution. The dried Fe3O4/TiO2 powder was then furnace-treated at 500 °C for 3 hours and characterized using XRD and UV-Vis. XRD results showed that the cubic crystal structure of Fe3O4 matched JCPDS No. 10–11032 in the 2θ range of 30.1°, 35.7°, 43.1°, 53.7°, and 57.2° with (hkl) planes of (220), (311), (400), (422), and (511). New diffraction peaks appeared at (101), (004), and (200), indicating the presence of TiO2 anatase phase crystals (JCPDS No. 21-1272). The calculated crystallite size decreased as the amount of TiO2 increased, due to the smaller atomic size of TiO2 compared to Fe3O4. This result indicates that Fe3O4/TiO2 synthesis was successfully achieved without altering the crystal structure. UV-Vis characterization with methylene blue at a wavelength of 663 nm showed differences in absorption values. The calculated band gap values using the Tauc Plot method increased from 2.36 to 2.38 eV. The degradation percentage of Fe3O4/TiO2 powder samples against methylene blue ranged from 99.55% to 99.38%. This result is consistent with the band gap values, where samples with lower band gaps demonstrated better degradation performance. The Fe3O4 material was successfully synthesized with TiO2, resulting in reduced band gap values and enhanced photocatalytic degradation capability of the Fe3O4/TiO2 nanocomposite.

Keywords: Photocatalyst, Fe3O4, TiO2, Moringa oleifera Leaves, Coprecipitation

INTRODUCTION

The advancement of human civilization, along with the rapid growth of technology and population, has led to an increase in pollution problems that threaten life on Earth. There has been a rise in pollutants from various sources

such as soil, water, and air (Nadimi et al., 2018).

All living organisms depend on water. Industrial activities have intensified environmental pollution due to the release of hazardous substances (Lendzion et al., 2020). Wastewater has become a major global issue,

particularly from industries such as textiles, printing, and manufacturing, each contributing significant amounts of waste. (Sari et al., 2023).

Methylene blue (MB) is a widely used organic dye for coloring textiles, wood, paper, plastics, and other materials. However, despite being categorized as an organic dye, excessive use of methylene blue can cause damage to human skin and eyes (Tumbelaka et al., 2022).

For the treatment of organic wastewater, photocatalytic photodegradation processes are preferred due to their environmentally friendly nature (Al-Nuaim et al., 2023). Photodegradation has been proven to be an effective method for the removal methylene blue (MB). Nevertheless, since organic pollutants in aqueous solutions cannot directly absorb solar energy, they cannot decompose on their own (Liu et al., 2020). Photocatalytic processes typically employ various materials such as TiO2, ZnO, Fe2O3, Fe3O4, CdS, GaP, ZnS, and WO3 (Tahir et al., 2020).

Solution for the recycling process is the use of magnetic materials (Fe3O4), which make TiO2 easier to separate from the solution. The incorporation of Fe3O4 can also modify the magnetic properties of TiO2 while simultaneously narrowing its band gap energy (Ramadhan et al., 2017). According to the study by Safeen et al. (2023), variations in calcination temperatures (300–1000 °C) affect the structural phase as well as the optical, dielectric, and photodegradation properties of nanoparticles.

Iron sand can be used as a raw material for the synthesis of Fe3O4 nanomaterials, which have wide-ranging technological applications. (Wicaksono et al., 2024). The synthesis of magnetic nanoparticles has largely relied on conventional methods, which have certain drawbacks, such as the use of toxic and expensive chemicals, as well as the generation of hazardous by-products. Therefore, there is a need for improved and eco-friendly methods to minimize the formation of new waste during nanoparticle synthesis, one of which is green synthesis (Tumbelaka et al., 2022).

Green synthesis is a method that produces nanoparticles using plant extracts (Sudarmono et al., 2024). This approach is clean, safe, cost-effective, and environmentally friendly (Huston et al., 2021). Many plants have been utilized in the synthesis of Fe3O4 nanoparticles, one of which is Moringa oleifera leaves, a member of the Moringaceae family. This tree is rich in nutrients and is often referred to as the 'miracle tree' (Virk et al., 2023).

Based on the above discussion, a green synthesis approach was carried out to produce Fe3O4/TiO2 photocatalyst materials using the coprecipitation method with Moringa oleifera leaf extract. This synthesis method reduces the side effects of chemical waste from conventional synthesis while providing materials with favorable characteristics.

RESEARCH METHOD

The Fe3O4/TiO2 photocatalyst material was synthesized using the coprecipitation method with the add of Moringa oleifera leaf extract as a natural reagent to reduce chemical waste from the synthesis process. This study involved several stages, including the preparation of moringa oleifera leaf extract, the synthesis of Fe3O4, and the green synthesis of Fe3O4/TiO2. The dried samples were then characterized using XRD and UV-Vis.

Preparation of Moringa oleifera Leaf Extract Solution

A total of 5 grams of Moringa oleifera leaf extract powder was dissolved in 60 ml of distilled water. The mixture was then stirred using a hot plate magnetic stirrer at 600 rpm for 1 hour at 60 °C. Subsequently, the solution was cooled to room temperature and filtered using filter paper to remove any extract residues. The filtrate obtained was stored in a refrigerator for use in the green synthesis process.

Synthesis of Fe3O4

A total of 25 grams of iron sand, previously extracted using an external magnet with three repetitions, was dissolved in 250 ml of 37% HCl. The mixture was stirred on a hot

Ridwan Yusuf Lubis, Abdul Halim Daulay, Masthura; Green-Synthesized Fe3O4/TiO2 Adsorption Material Via Coprecipitation Method Using Moringa Oleifera Leaf Extract for the Degradation of Methylene Blue

plate magnetic stirrer for 30 minutes at 520 rpm and 70 °C. The solution was then allowed to settle at room temperature overnight in a dark room. The residue of the iron sand was filtered using filter paper to obtain FeCl3 solution. The filtrate was subsequently titrated with NaOH until reaching pH 10, while stirring for 30 minutes at 70 °C and 520 rpm. The Fe3O4 precipitate formed in the solution was then dried in an oven at 120 °C for 6 hours.

Green Synthesized Fe3O4/TiO2

A total of 4 grams of Fe3O4 powder was mixed with 10 ml of ethanol and stirred using a hot plate magnetic stirrer for 30 minutes at room temperature. The mass composition ratios of Fe3O4/TiO2 used were FTMO1:2, FTMO1:1, and FTMO2:1. TTIP and the Moringa oleifera leaf extract solution were mixed and stirred for 1 hour at 700 rpm. Subsequently, the Fe3O4 solution, TTIP, and leaf extract were combined and stirred at 700 rpm for 1 hour. The precipitate formed in the solution was separated using an external magnet and washed seven times until neutral pH was reached. The sample was then dried in an oven at 120 °C for 2 hours, followed by furnace treatment at 500 °C for 3 hours.

X-Ray Diffraction (XRD) Characterization

The XRD test results were analyzed to determine the phases and crystal structures of the samples. The analysis focused on phase changes and crystallite size variations resulting from temperature treatment and different mass ratios used in the study. The X-ray source employed was CuK α radiation with a wavelength of $\lambda = 1.54$ Å.

Ultraviolet-Visible Spectroscopy (UV-Vis) Characterization

UV-Vis characterization was conducted to analyze the surface area of activated carbon using a methylene blue solution. A total of 1 g of solid methylene blue was dissolved in 1000 mL of water to obtain a 1000 ppm methylene blue solution. The concentration was then adjusted using the following equation:

$$v_1 \times M_1 = v_2 \times M_2$$

Volumes of 0, 0.25, 0.5, 0.8, and 1 mL of the 1000 ppm methylene blue solution were each diluted with 50 mL of distilled water to obtain MB concentrations of 0, 5, 10, 16, and 20 ppm, respectively. The active sample was then mixed into the 16 ppm MB solution and analyzed using UV-Vis at a wavelength of 663 nm.

RESULT AND DISCUSSION

Results

The Fe3O4/TiO2 photocatalyst material synthesized via the coprecipitation method using Moringa oleifera leaf extract was characterized using XRD and UV-Vis.

XRD Characterization

The characterization results using XRD were plotted into a graph using Origin software, as shown in Figure 1. The samples used in this study utilized three mass variations. Based on the XRD test results in Figure 1, the diffractogram peak data was obtained and analyzed using Match! Crystal **Impact** software. The diffractogram shows diffraction peaks at a 20 angle ranging from 10° to 80°. The crystal structure formed is cubic with peak angles 20 at 30.10, 35.7 o, 43.10, 53.7 o, and 57.2 o, and crystal planes (hkl) of (220), (311), (400), (422), and (511). This result is consistent with the JCPDS card No. 10-11032 for Fe3O4 and the peak angle of the TiO2 anatase phase JCPDS card No. 21-1272 (Tumbaleka et al., 2021).

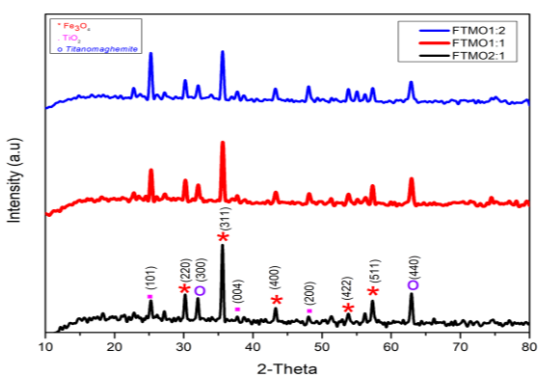


Figure 1. Difraktogram XRD of Fe3O4/TiO2

Several 2θ peak angles also indicate the presence of the Fe2O4TiO2 compound with a Titanomaghemite phase, which has a cubic structure based on analysis from the Match! Crystal Impact software. The presence of several compounds detected at the XRD diffractogram

peaks have different dhkl values, as shown in Table 1. This indicates that the Fe3O4 compound has the smallest dhkl value, suggesting it is the least abundant compound in the sample.

Table 1. Value of dhkl Fe3O4, TiO2 dan Titanomaghemite

Compound	dhkl (Å)	a (Å)
Fe ₃ O ₄	2,51	8.34
TiO_2	3,51	3.78
Titanomaghemite	2,78	8.34

The smaller the dhkl value, the denser the atoms of that compound. The analysis from the Match! Crystal Impact software shows the percentages: Fe3O4 at 26.8%, TiO2 at 40.7%, and Titanomaghemite at 32.5%.

Further analysis was performed by analyzing the diffractogram peak at an angle of 35.7° with a Miller index (hkl) analysis of (311), which can be seen in Figure 2.

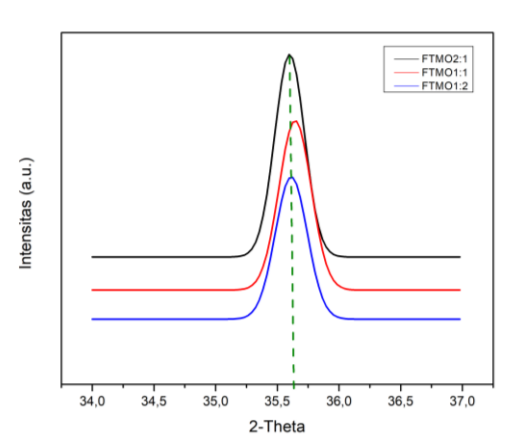


Figure 2. Graph of the Peak Shift at the 35.7°

An increase in intensity occurred in the Fe3O4/TiO2 sample, indicating an improvement in crystal quality after Fe3O4 was composited with the TiO2 material. This happened because some of the atoms belonging to Fe3O4 bonded with TiO2 atoms, which is a non-magnetic material. This bonding makes the atoms more ordered, which consequently leads to an increase in crystal quality (Fauzi., 2023)

The result of the crystal size calculation using the Debye-Scherrer equation :

$$D = \frac{K\lambda}{\beta \cos \theta}$$

Table 2. Crystal Size Fe3O4/TiO2

Sample	FWHM	D (nm)
	(radian)	D (nm)

FTMO2:1	0,28373	30,71
FTMO1:1	0,30705	28,59
FTMO1:2	0,30472	28,38

This explains that the FTMO2:1 sample has a larger crystal size value than FTMO1:1 and FTMO1:2, but the change in crystal size is not very significant. The effect of mass variation influences the crystal size value, which can be seen by the decreasing crystal size value as the mass variation of TiO2 increases. In a larger crystal size, atoms tend to be more ordered because the crystal grows with fewer defects. The larger the crystal, the more regular the arrangement of atoms within it. This is because when the mass variation is higher, the atoms in the TiO2 compound will diffuse rapidly (Ilmi., 2020).

UV-Vis Characterization

UV-Vis is a tool used to measure light absorbance and determine the energy gap value. In this research, samples with codes FTMO2:1, FTMO1:1, and FTMO1:2 were analyzed in the 500–900 nm wavelength range, which is the range for visible light, because the absorption of Methylene Blue at a concentration of 10 ppm occurs at a wavelength of 663 nm.

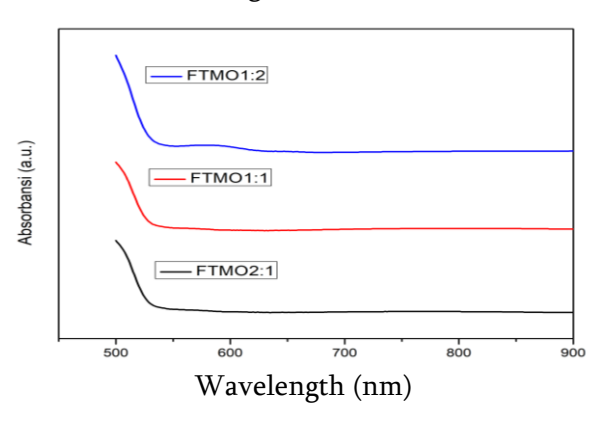


Figure 3. Spectrum UV-Vis Fe3O4/TiO2

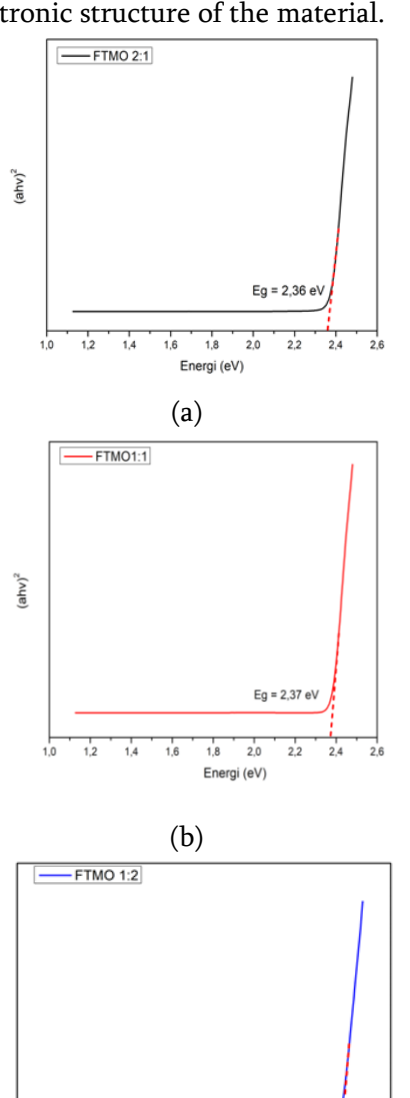
Figure 3. of the UV-Vis test above shows the absorption peak spectrum and the absorption edge of the Fe3O4/TiO2 nanocomposite (Fauzi., 2023). A wavelength shift occurred, which is mostly caused by a change in particle size. The charge transfer transition between the Fe3O4 nanoparticle electrons and the conduction band (or valence band) of TiO2 can explain the shift in the absorption band. This indicates that all nanoparticle samples absorb visible light

Ridwan Yusuf Lubis, Abdul Halim Daulay, Masthura; Green-Synthesized Fe3O4/TiO2 Adsorption Material Via Coprecipitation Method Using Moringa Oleifera Leaf Extract for the Degradation of Methylene Blue

between the wavelengths of 500 nm to 550 nm (Tumbelaka et al., 2021).

The absorption curve tends to be stable up to the 900 nm range. However, the absorbance intensity of each sample varies, with samples FTMO2:1 and FTMO1:1 having the lowest absorbance, which indicates that these materials have a smaller capacity to absorb light.

This difference in intensity is caused by the mass variation of the constituent materials of FTMO, where a larger or smaller mass variation influences the intermolecular interactions and the electronic structure of the material.



(c) **Figure 4.** Bandgap energy value (a) FTMO2:1,
(b) FTMO1:1 and (c) FTMO1:2.

Energi (eV)

(ahv)²

The Tauc Plot Method is carried out by drawing a linear line between the y and x axes. A straight line is drawn between the

multiplication of the absorbed energy (hv) and the absorption coefficient (α hv)2, until it intercepts the energy axis, and the energy gap value is obtained. After creating the graph showing the relationship between hv and (α hv)2, a line is drawn tangent to the inflection point on the curve (Crismeli., 2024). Figure 4. presents the energy gap of each sample.

The energy gap values for each sample can be seen in Table 3 below :

Table 3. Energy Gap Fe3O4/TiO2

	67 1
Sample	Energy Gap (eV)
FTMO2:1	2,36
FTMO1:1	2,37
FTMO1:2	2,38

The data above can be summarized as follows: this result is consistent with that reported by (Tumbeleka et al., 2022). The increase in the energy band gap is highly correlated with the crystallite size results from the XRD analysis; when the particle size decreases, the energy band gap increases.

With the increase of energy band gap, a greater amount of energy is required to excite electrons to the conduction band. Even so, an increased bandgap means that electron-hole recombination will not be too fast, thereby enhancing the process of photodegradation of dye waste (Fauzi., 2023).

The smaller particle size, the valence band and conduction band more shift away from each other, resulting in a larger gap between the valence band and the conduction band of the material (Syafrian and Hary., 2024).

Percentage degradation of Methylene Blue can be used as an indicator of the change in the energy gap, which can be calculated using Equation below to obtain the values shown in Table 4.

Degradation (%)=
$$\left(\frac{c_0-c_t}{c_0}\right) \times 100 \%$$

Based on Table 4.4, the absorbance of Methylene Blue at 10 ppm decreased from an initial value of 2.029 wavelength of 663 nm to 0.062 (FTMO2:1), 0.057 (FTMO1:1), and 0.045 (FTMO1:2). The absorption efficiency for each

sample was 99.38%, 99.43%, and 99.55%, respectively.

Table 4. Percentage of Degradation

_			- 6
_	Sample	Absorbance UV-Vis 663 (nm)	Degradation (%)
-	FTMO2:1	0,062	99,38
	FTMO1:1	0,057	99,43
	FTMO1:2	0,045	99,55

CONCLUSION AND SUGGESTION

This research successfully synthesized Fe₃O₄/TiO₂ photocatalyst material using the coprecipitation method with the assistance of Moringa oleifera leaf extract as an eco-friendly agent. XRD analysis revealed that the Fe₃O₄ crystal structure remained preserved after being composited with TiO2, with the formation of the anatase TiO2 phase that supports photocatalytic properties. UV-Vis analysis confirmed that the bandgap value increased from 2.36 eV to 2.38 eV with the addition of TiO2, which is associated with a reduction in crystallite size. The degradation capability of Methylene Blue (MB) dye reached a high efficiency of 99.38-99.55%. These results indicate that the synthesized nanocomposite material exhibits excellent performance as an eco-friendly photocatalyst for wastewater treatment, particularly for textile industry effluents containing organic dyes.

REFERENCES

- Al-Nuaim, A., Al-Mubaddel, F. S., & Al-Zahrani, S. M. (2023). Photodegradation of organic pollutants using advanced photocatalytic processes: A review. Journal of Environmental Chemical Engineering, 11(2), 109–121.
- Crismeli, A. (2024). Application of Tauc plot analysis for optical band gap determination. Materials Science Reports, 12(1), 45–56.
- Fauzi, A. (2023). Crystal structure and optical properties of Fe-based nanomaterials. Journal of Materials Research, 15(4), 203–212.
- Huston, S., Lee, D., & Kumar, R. (2021). Green synthesis of nanoparticles using plant extracts:A sustainable approach. Journal of Nanoscience and Nanotechnology, 21(3),

- 1001-1010.
- Ilmi, R. (2020). Effect of TiO2 variation on crystallite size and band gap in nanocomposites. International Journal of Materials Physics, 7(2), 88–95.
- Lendzion, J., Kowalski, T., & Nowak, M. (2020). Industrial wastewater pollution and treatment technologies: A review. Environmental Protection Engineering, 46(1), 15–28.
- Liu, J., Zhao, Y., & Chen, H. (2020). Mechanism of methylene blue photodegradation using semiconductor catalysts. Journal of Environmental Sciences, 89, 35–46.
- Nadimi, M., Karimi, B., & Alavi, S. (2018). Environmental pollution and its impacts on ecosystem sustainability. Ecological Indicators, 93, 105–112.
- Ramadhan, A., Sutanto, H., & Wirawan, F. (2017). Effect of Fe3O4 incorporation on the photocatalytic performance of TiO2. Materials Chemistry and Physics, 196, 1–9.
- Safeen, S., Ahmed, A., & Khan, M. (2023). Effect of calcination temperature on structural and optical properties of TiO2 nanoparticles. Journal of Physics and Chemistry of Solids, 176, 110–118.
- Sari, D., Nugraha, A., & Putri, L. (2023). Industrial wastewater management and environmental sustainability. International Journal of Environmental Research, 20(5), 250–265.
- Sudarmono, D., Putra, H., & Siregar, A. (2024). Advances in green synthesis of magnetic nanoparticles using plant extracts. Green Chemistry Letters and Reviews, 17(1), 77–89.
- Syafrian, A., & Hary, R. (2024). Band gap engineering in Fe-Ti nanocomposites for enhanced photocatalysis. Materials Today: Proceedings, 72, 455–462.
- Tahir, A., Rahman, M., & Abbas, G. (2020). Review of photocatalytic materials for wastewater treatment applications. Applied Catalysis B: Environmental, 270, 118–125.
- Tumbelaka, F., Santoso, A., & Yusuf, M. (2021). Structural analysis of Fe3O4/TiO2 nanocomposites. Materials Research Express,

Ridwan Yusuf Lubis, Abdul Halim Daulay, Masthura; Green-Synthesized Fe3O4/TiO2 Adsorption Material Via Coprecipitation Method Using Moringa Oleifera Leaf Extract for the Degradation of Methylene Blue

8(5), 551–563.

- Tumbelaka, F., Santoso, A., & Yusuf, M. (2022). Photodegradation performance of greensynthesized nanomaterials. Journal of Environmental Nanotechnology, 11(3), 199–210.
- Virk, R., Singh, A., & Kumar, V. (2023). Moringa oleifera: A multifunctional tree for nutrition and nanomaterial synthesis. Plant-Based Nanotechnology, 9(2), 101–115.
- Wicaksono, A., Putra, D., & Lestari, S. (2024). Iron sand as a raw material for Fe3O4 nanoparticles: A review. Indonesian Journal of Materials Science, 15(1), 33–42.